Multifrequency electron paramagnetic resonance of Ce^{3+} in the $Gd(HBPz_3)_2$ tropolonate complex: high-field effects

2005 J. Phys.: Condens. Matter 17 5563

(http://iopscience.iop.org/0953-8984/17/36/012)

INSTITUTE OF PHYSICS PUBLISHING JOURNAL OF PHYSICS: CONDENSED MATTER

J. Phys.: Condens. Matter **17** (2005) 5563–5575 doi:10.1088/0953-8984/17/36/012

Multifrequency electron paramagnetic resonance of Ce^{3+} in the $Gd(HBPz_3)_2$ tropolonate complex: high-field effects

F F Popescu[1,5], M Martinelli[2], C A Massa[2], L A Pardi[2] and V Bercu[2,3,4]

[1] Department of Physics, University of Bucharest, Magurele, Ro-76900, Bucharest, Romania
[2] Istituto per i Processi Chimico-Fisici, CNR, via G Moruzzi 1, 56124 Pisa, Italy
[3] Dipartimento di Fisica 'Enrico Fermi', Università di Pisa, Largo Bruno Pontecorvo 3, I-56127 Pisa, Italy
[4] INFM UdR Pisa, Largo Bruno Pontecorvo 3, I-56127 Pisa, Italy

E-mail: ffpopescu@k.ro

Received 4 May 2005, in final form 8 August 2005
Published 26 August 2005
Online at stacks.iop.org/JPhysCM/17/5563

Abstract

An electron paramagnetic resonance (EPR) powder spectrum investigation of rare earth trace impurities in the $Gd(HBPz_3)_2$ tropolonate complex (GdTrp) was carried out at 95, 190, and 285 GHz. Ce^{3+} ion impurities were identified by EPR transitions between levels of the two lowest-lying doublets of the ground $J = 5/2$ manifold. An important frequency and magnetic-field dependence of the g-factor was observed. The system was successfully described by a Hamiltonian appropriate for tetragonal symmetry without orthorhombic distortion. Compared to conventional microwave EPR spectroscopy, at high fields these effective g-values depend not only on the polar angle between the magnetic field **B** and the tetragonal axis, but also on the azimuthal angle φ between **B** and the binary axes of the molecular complex. These dependences include additional terms proportional to $(B)^{2m}(\cos 4\varphi)^n$, where $m \geqslant n$ are natural numbers. They show that in the present experiment, the Zeeman interaction is comparable with the zero-field splitting of the ground manifold. It is found that the second, and the third doublet are located at $13.98 \pm 0.25\ \mathrm{cm}^{-1}$ and $9.32 \pm 0.15\ \mathrm{cm}^{-1}$ above the first one, respectively.

1. Introduction

Complexes of rare earth ions, which can provide very high spin and large anisotropy, are attracting increasing interest in the field of molecular magnetism. Complexes of lanthanide ions with different paramagnetic building blocks, ranging from metal ions to radical ligands, have recently been reported [1]. The lanthanide ions are usually involved in weak exchange coupling

[5] Author to whom any correspondence should be addressed.

interactions, whose magnitude is comparable with the crystal-field splitting of the ground J multiplet. The experimental approach to separate the different contributions of crystal field and exchange coupling to the magnetic properties in either heterometallic or lanthanide-radical complexes involves the determination of magnetic properties of a corresponding complex in which the second spin carrier is substituted by a diamagnetic analogue giving rise to comparable ligand field effects on the metal ion. This strategy of diamagnetic substitution was used for example in the homologous series of compounds $Ln(DTBSQ)(HBPz_3)_2$ and $Ln(Trp)(HBPz_3)_2$ by replacing the paramagnetic semiquinone ligand with the diamagnetic tropolonato ligand [1, 2]. Within this experimental approach, the exchange interaction was estimated by subtracting from the magnetic susceptibilities of the exchange coupled complexes the temperature-dependent contribution arising from the thermal depopulation of the excited levels of the ground J multiplet. However, the magnetic susceptibility measurements may not be the best way to locate these excited levels [1]. Since the differences between the energy levels of the ground J multiplet are small, it is difficult to obtain them from optical measurements. At low temperature, conventional microwave electron paramagnetic resonance (EPR) spectroscopy detects signals attributed to the ground doublet. In such a situation no further information can be derived from the EPR results, since the number of relevant crystal-field parameters, from which the g-matrix components could eventually be derived, is too high [3, 4]. Due to the fast relaxation and low sensitivity, the presence of low-lying excited doublets is also difficult to be evidenced by conventional EPR spectroscopy.

However, the Zeeman interaction may admix doublet states of the ground J manifold. If the Zeeman interaction is not very small in comparison with the crystal-field splitting of the ground J multiplet, the effective g-matrix components of the doublets may have important magnetic-field dependences [3]. Therefore, high-field EPR spectroscopy (HF-EPR) could be used to obtain the zero-field splitting of the ground J manifold. For example, in tetragonal symmetry, at low fields, the g-tensor shows only two diagonal values corresponding to the axial case $g_z = g_\parallel$ and $g_x = g_y = g_\perp$ which are magnetic-field independent [3, 4]. In high fields, the effective g-components become magnetic-field dependent. In addition, we will show that although $g_x = g_y$, the effective $g_\perp$-component exhibits azimuthal angular dependence. In powder spectra this angular dependence splits the perpendicular transition, even in the axial case. On increasing the magnetic resonance field of this transition by increasing the frequency of the far-infrared quanta, the perpendicular EPR line become split into two components corresponding to $\varphi = 0, \pm\frac{\pi}{2}$ and $\varphi = \pm\frac{\pi}{4}$, respectively. This splitting is proportional to $\cos 4\varphi$, where φ is the angle between the magnetic-field component perpendicular to the tetragonal axis and one of the two equivalent binary axes. By increasing the magnetic field, the splitting becomes proportional to $\frac{B^3}{(\Delta E_i^0)^2}$, where ΔE_i^0 is the zero-field splitting of the J ground manifold. On continuing to increase the frequency and the magnetic-field intensity, the splitting of the line position depends on other supplementary terms proportional to $\frac{B^5}{(\Delta E_i^0)^4}$, $\frac{B^7}{(\Delta E_i^0)^6}$ and so on. The second splitting corresponds to $\varphi = 0, \pm\frac{\pi}{2}, \pm\frac{\pi}{4}$, and $\varphi = \pm\frac{\pi}{8}$, respectively. It is proportional to $\cos^2 4\varphi$.

The main aim of this paper is to show that the multifrequency HF-EPR spectra of Ce^{3+} trace impurities in the $Gd(HBPz_3)_2$ tropolonate complex (GdTrp) exhibit important magnetic-field and azimuthal angular dependences of the effective g-matrix components. These dependences allow us to find, with a good approximation, the crystal-field splitting of the $J = \frac{5}{2}$ manifold of the Ce^{3+} in GdTrp. This method of finding the crystal-field splitting was verified by detecting an EPR transition between the ground doublet and the low-lying excited doublet, since the line position of this transition allows us to find the energy difference between the corresponding doublets directly.

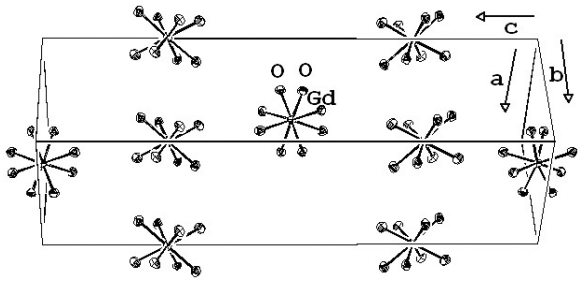

Figure 1. Simplified GdTrp crystal structure showing the unit cell content.

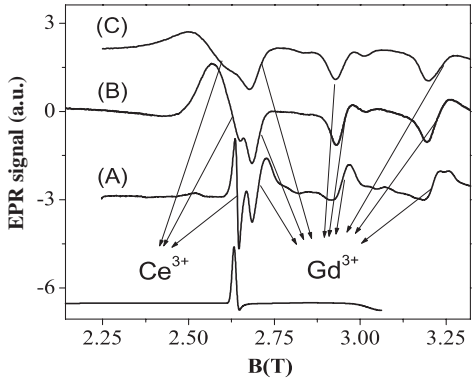

Figure 2. The parallel transition of Ce^{3+} trace impurities in GdTrp at 95 GHz and 4.2 K. The lower spectrum is the simulated one and the upper spectra (A), (B) and (C) are experimental spectra obtained on powder samples whose size of grains decreases by milling.

2. The experimental results

The EPR measurements were performed at 95, 190, and 285 GHz, with an EPR spectrometer described in [5]. The molecular structure of LnTrp is described elsewhere [1]. For Ln = Ho^{3+}, the structure was successfully refined; the Eu^{3+}, Er^{3+}, and Gd^{3+} derivatives were assumed to be isostructural on the basis of the cell parameters. GdTrp crystallizes in the tetragonal system. It is a molecular complex in which the Gd^{3+} ion is coordinated to eight atoms forming a square antiprism. Out of these, six are nitrogen atoms coming from two $HBPz_3$ molecules and two are the oxygen atoms of the Trp molecule. A simplified version of the crystal structure of GdTrp is reported in figure 1, showing the Gd ions in the unit cell with their first coordination sphere. For the sake of clarity only the two oxygen atoms coming from the Trp moieties are labelled in figure 1, the other atoms being the nitrogen atoms of the HBz_3 molecules. The long axis is the tetragonal c-axis and the two short axes are the binary axes a and b. The conventional X-band EPR, and HF-EPR powder spectra of Gd^{3+} in GdTrp have been studied elsewhere [2, 6]. Besides the Gd^{3+} spectrum, at liquid helium temperature the EPR spectrum of GdTrp exhibits some additional lines. For example, at 95 GHz, between 2.6 and 4.1 T there are intense lines due to the allowed $\Delta M = \pm 1$ transitions and some weak transitions around 1.7 T corresponding to the forbidden transitions $\Delta M = \pm 2$ of Gd^{3+}. All these transitions can be detected at any temperature. At liquid helium temperature, there are three other transitions at 2.570, 4.409 and 4.648 T. Their lineshapes (see figures 2 and 3) are characteristic of the powder spectrum of a paramagnetic centre with an effective spin $1/2$. The effective g-values

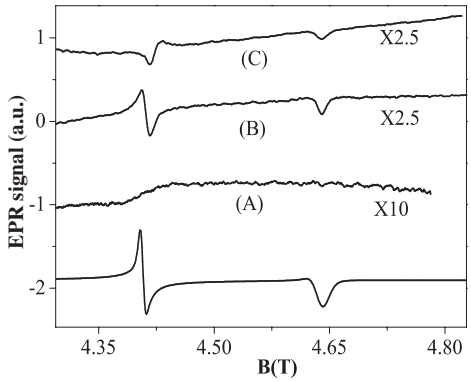

Figure 3. The perpendicular transitions of Ce^{3+} trace impurities in GdTrp at 95 GHz and 4.2 K, multiplied by a factor specified in the figure.

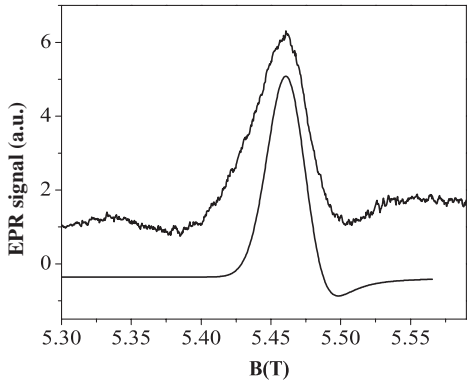

Figure 4. The parallel transition of the ground doublet of Ce^{3+} trace impurities in GdTrp at 190 GHz and 4.2 K. The lower spectrum is the simulated one and the upper spectrum is the experimental one.

attributed to the above three transitions are 2.646 ± 0.005, 1.545 ± 0.004 and 1.466 ± 0.004, respectively. The fact that this centre is observed only at liquid helium temperature shows that it must have a short spin-lattice relaxation time, in agreement with rare earth ions characterized by an effective spin one-half. In addition, these lines do not exhibit hyperfine components. From these observations it was concluded that the rare earth trace impurity responsible for these signals is Ce^{3+} [3, 4]. The effective g-values mentioned above are similar to those of tetragonal Ce^{3+} centres in other crystals [4, 7], and especially in several scheelite compounds [8]. In our case, the three g-values seem to be consistent with an almost axial spectrum characterized by a tetragonal symmetry with a small orthorhombic distortion. At 190 GHz, the three transitions described above are expected to be observed at magnetic fields two times larger than those detected at 95 GHz. Within the limit of experimental errors, although our spectrometer has the best sensitivity at 190 GHz, the two transitions at higher fields are not detected, while the lower-field transition is observed at 5.475 T ($g = 2.484$) instead of 5.15 T (see figure 4). In addition, another transition is observed at 4.555 T (see figure 5). At 285 GHz, only the lower-field transition is detected but at 9.21 T ($g = 2.215$) instead of 7.725 T (see figure 6). We cannot make any experimental remark on the higher-field transitions at 285 GHz, because the upper limit of the magnetic field is 12 T. Consequently, the experiment shows that at least

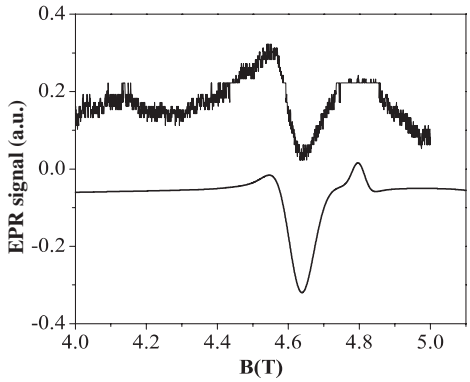

Figure 5. The parallel transition illustrated in figure 7, between the ground doublet and the first excited doublet of the Ce^{3+} ground multiplet in GdTrp at 190 GHz and 4.2 K. The lower spectrum is the simulated one and the upper spectrum is the experimental one.

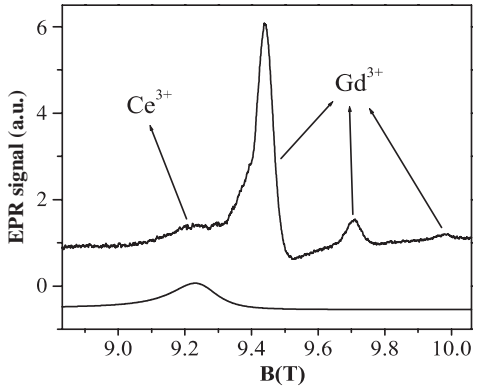

Figure 6. The parallel transition of the ground doublet of Ce^{3+} trace impurities in GdTrp at 285 GHz and 4.2 K. The lower spectrum is the simulated one and the upper spectrum is the experimental one.

the effective g-value of the lower-field transition has an important magnetic-field dependence, decreasing with increasing the frequency. This fact suggests that the lowest doublet of the ground $J = 5/2$ manifold of the Ce^{3+} cannot be considered well isolated at the mentioned high-field, and that the crystal-field splitting of the ground multiplet is comparable with the Zeeman interaction.

3. High-field effects in the EPR spectrum of the $^2F_{5/2}$ ground multiplet

The electronic configuration of Ce^{3+} is $4f^1$ with ground state $^2F_{5/2}$. Ce^{3+} cannot be identified by a hyperfine interaction because all isotopes have no nuclear spin. The first excited state is $^2F_{7/2}$, situated at about 2000 cm^{-1} above the ground state. Consequently, although some theoretical studies consider a slight admixture from the $J = 7/2$ excited state [7, 9], to a good approximation, we can consider the ground state $^2F_{5/2}$ well isolated. In tetragonal symmetry this ground state is split into three Kramers doublets. Since the experiment suggests that the Zeeman interaction may be comparable with the crystal-field splitting of the ground multiplet,

we consider the following Hamiltonian the most appropriate:

$$H = \beta \mathbf{J} g_J \mathbf{B} + H_{\text{cryst}}, \tag{1}$$

where the first term represents the Zeeman interaction. For the Ce^{3+} free ion g_J is a constant: $g_J = g_L$, where $g_L = 6/7$ is the Landé factor of the ground state $^2F_{5/2}$. In practice, in order to calculate the effective g-values, g_J does not correspond exactly to g_L [10–12]. That is why we consider g_J a matrix in equation (1), although the diagonal values of this matrix are expected to be close to g_L. In addition, because the symmetry is lower than cubic, the Zeeman interaction in equation (1) was not considered isotropic.

The second term represents the crystal-field interaction. For tetragonal symmetry with an orthorhombic distortion corresponding to a ground state $^2F_{5/2}$,

$$H_{\text{cryst}} = B_2^0 O_2^0 + B_2^2 O_2^2 + B_4^0 O_4^0 + B_4^4 O_4^4. \tag{2}$$

A program written by Weihe [13] was used to generate the powder EPR spectra. It allows direct assignment of the observed lineshape of the EPR transitions by considering Lorentzian or Gaussian lineshapes of the individual crystallites, and a Gaussian distribution of the spin-Hamiltonian parameters. The best simulation of the six observed transitions mentioned in the previous section (see figures 2–6) attributed to Ce^{3+} are obtained with the following values of the above Hamiltonian parameters: $g_J^z = g_J^{\parallel} = 0.810 \pm 0.005$; $g_J^x = g_J^y = g_J^{\perp} = 0.825 \pm 0.005$; $B_2^0 = (-0.400 \pm 0.006)\,\text{cm}^{-1}$; $B_2^2 = (0.000 \pm 0.006)\,\text{cm}^{-1}$; $B_4^0 = (-0.013\,73 \pm 0.000\,30)\ \text{cm}^{-1}$; $|B_4^4| = (0.2124 \pm 0.0020)\ \text{cm}^{-1}$.

Since B_2^2 is zero within errors, the above parameters correspond to a tetragonal symmetry without or with a very small orthorhombic distortion. For an axial powder spectrum there are two types of transitions: the first type corresponds to the magnetic field **B** parallel to the tetragonal axis, and the second type to **B** perpendicular to this axis.

3.1. High-field effects of the parallel transition

At this orientation of the magnetic field, for a state $^2F_{5/2}$ characterized by a tetragonal symmetry without orthorhombic distortion, exact solutions of the Hamiltonian can be obtained (see equation (1)). They are similar to those corresponding to cubic symmetry with tetragonal distortion [14]. The energy eigenvalues and the corresponding eigenstates are given by

$$E_{1,\parallel}^{1,2} = \tfrac{1}{2}(C_0^{5/2} + C_0^{3/2} \mp g_J^{\parallel}\beta B) - \tfrac{1}{2}\sqrt{(\Delta C_0 \mp 4 g_J^{\parallel}\beta B)^2 + (2C_4)^2}, \tag{3}$$

$$E_{2,\parallel}^{1,2} = \tfrac{1}{2}(C_0^{5/2} + C_0^{3/2} \mp g_J^{\parallel}\beta B) + \tfrac{1}{2}\sqrt{(\Delta C_0 \mp 4 g_J^{\parallel}\beta B)^2 + (2C_4)^2}, \tag{4}$$

$$E_{3,\parallel}^{1,2} = C_0^{1/2} \mp \tfrac{1}{2} g_J^{\parallel}\beta B, \tag{5}$$

$$\Psi_{1,\parallel}^{1,2} = p_{1,2}\left|\mp\tfrac{5}{2}\right\rangle + q_{1,2}\left|\pm\tfrac{3}{2}\right\rangle, \tag{6}$$

$$\Psi_{2,\parallel}^{1,2} = q_{1,2}\left|\mp\tfrac{5}{2}\right\rangle - p_{1,2}\left|\pm\tfrac{3}{2}\right\rangle, \tag{7}$$

$$\Psi_{3,\parallel}^{1,2} = \left|\mp\tfrac{1}{2}\right\rangle, \tag{8}$$

with

$$p_{1,2}^2 = \frac{1}{2}\left(1 - \frac{\Delta C_0 \mp 4 g_J^{\parallel}\beta B}{\sqrt{(\Delta C_0 \mp 4 g_J^{\parallel}\beta B)^2 + (2C_4)^2}}\right), \tag{9}$$

$$q_{1,2}^2 = \frac{1}{2}\left(1 + \frac{\Delta C_0 \mp 4 g_J^{\parallel}\beta B}{\sqrt{(\Delta C_0 \mp 4 g_J^{\parallel}\beta B)^2 + (2C_4)^2}}\right), \tag{10}$$

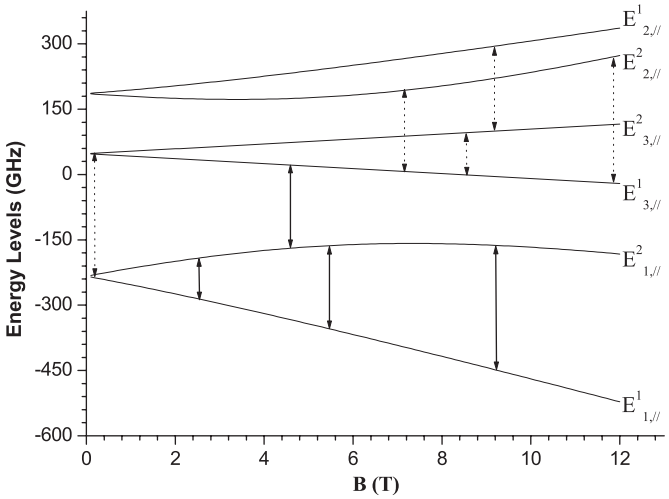

Figure 7. Energy level diagram for magnetic field B parallel to the z-axis of the ground $J = 5/2$ multiplet of Ce^{3+} in GdTrp, and the allowed parallel HF–EPR transition at 95, 190 and 285 GHz. Solid line: observed transition; dashed line: other possible allowed transition.

where $C_0^{|M|} = \langle \pm M|H_{\rm cryst}|\pm M\rangle$; $\Delta C_0 = C_0^{5/2} - C_0^{3/2}$; $C_4 = \langle \mp\frac{5}{2}|H_{\rm cryst}|\pm\frac{3}{2}\rangle$. As one can see, the Zeeman interaction changes the admixture between the $|\mp\frac{5}{2}\rangle$ and $|\mp\frac{3}{2}\rangle$ doublets of the free Ce^{3+} ion due to the crystal field. For the corresponding mixed states, the line position of the parallel-type transition depends on ΔC_0, $2C_4$ and $h\nu$ which is the far-infrared quantum. By using the crystal-field parameters obtained with Weihe's program, one obtains $\Delta C_0 = -8.1\ \mathrm{cm}^{-1}$, and $|2C_4| = 11.4\ \mathrm{cm}^{-1}$. At conventional microwave EPR frequencies $4g_J^{\parallel}\beta B \ll \Delta C_0, 2C_4$. Consequently, at low fields the effective g-value is

$$(g_0^{\parallel})_1 = g_J^{\parallel}\left(1 + \frac{4}{\sqrt{1 + (\frac{2C_4}{\Delta C_0})^2}}\right) = 2.686. \tag{11}$$

At conventional microwave frequencies the line position of the parallel transition depends only on $g_0^{\parallel}$. Thus the three parameters ΔC_0, $2C_4$ and $g_J^{\parallel}$ cannot be found independently with conventional EPR spectroscopy. As one can see at $\nu = 95$, 190, or 285 GHz, $h\nu$ is comparable with ΔC_0, and $2C_4$. At these frequencies the line position of the parallel transition depends also on $h\nu$ and B. The magnetic-field dependences of the energy levels of the ground manifold of Ce^{3+} in GdTrp for magnetic field parallel to the tetragonal axis are illustrated in figure 7. Full lines represent the observed EPR transitions at the three frequencies mentioned above. The parallel-type transitions between the two levels of the ground doublet at these frequencies allow us to find the parameters ΔC_0, $2C_4$, $g_J^{\parallel}$, and the zero-field splitting between the two doublets:

$$E_2^0 - E_1^0 = \sqrt{\Delta C_0^2 + (2C_4)^2} = (13.98 \pm 0.25)\ \mathrm{cm}^{-1}. \tag{12}$$

The crystal-field splitting $E_3^0 - E_1^0$ cannot be found using the parallel-type transition of the ground doublet, because in tetragonal symmetry the states $|\mp\frac{1}{2}\rangle$ are not mixed with the states $|\mp\frac{5}{2}\rangle$, or $|\mp\frac{3}{2}\rangle$ by the crystal field, or the Zeeman interaction. Fortunately, at 190 GHz another parallel type transition is observed between the ground doublet and the first excited doublet (see figure 5). The line position of this transition allows us to measure the zero-field

splitting $E_3^0 - E_1^0$ directly:

$$E_3^0 - E_1^0 = C_0^{1/2} - \tfrac{1}{2}(C_0^{3/2+}C_0^{5/2}) + \tfrac{1}{2}\sqrt{\Delta C_0^2 + (2C_4)^2} = (9.32 \pm 0.15)\ \mathrm{cm}^{-1}. \tag{13}$$

3.2. High-field effects of the perpendicular transitions

If the magnetic field is perpendicular to the tetragonal axis, the secular equation of the Hamiltonian (equation (1)) is

$$\begin{aligned}\{&(E_1^0 - E_\perp)(E_2^0 - E_\perp)(E_3^0 - E_\perp) - [2p_0^2(E_1^0 - E_\perp) + 2q_0^2(E_2^0 - E_\perp) \\ &+ \tfrac{5}{4}(E_3^0 - E_\perp)](g_J^\perp \beta B)^2\}^2 - \left\{\left(\tfrac{3}{2}\right)^2\left[(E_1^0 - E_\perp)(E_2^0 - E_\perp) - \tfrac{5}{4}(g_J^\perp \beta B)^2\right]^2\right. \\ &\left. + 5p_0^2q_0^2(E_1^0 - E_2^0)^2\left[(E_3^0 - E_\perp)^2 - \left(\tfrac{3}{2}g_J^\perp \beta B\right)^2\right]\right\} \\ &\times (g_J^\perp \beta B)^2 + 6\sqrt{5}p_0q_0(E_1^0 - E_2^0)[p_0^2(E_1^0 - E_\perp) \\ &+ q_0^2(E_2^0 - E_\perp)](g_J^\perp \beta B)^4 \cos 4\varphi = 0\end{aligned} \tag{14}$$

where p_0 and q_0 are the mixing coefficients given by equations (9) and (10) for $B = 0$, and φ is the angle between **B** and one of the two binary axes x and y.

In contrast to the parallel case, the above equation does not have analytical solutions. However, for the energy levels of the corresponding three doublets, the solutions must have the following magnetic-field dependence:

$$\begin{aligned}E_{i,\perp}^{1,2} = E_i^0 &\mp \tfrac{1}{2}(g_\perp^0)_i \beta B - \alpha_i (g_J^\perp \beta B)^2 \mp (\varepsilon_i + \varepsilon_i^\varphi \cos 4\varphi)(g_J^\perp \beta B)^3 \\ &- (\gamma_i + \gamma_i^\varphi \cos 4\varphi)(g_J^\perp \beta B)^4 \\ &\mp \left(\eta_i + \eta_i^\varphi \cos 4\varphi - \frac{(\varepsilon_i^\varphi)^2 g_J^\perp}{(g_\perp^0)_i}\cos^2 4\varphi\right)(g_J^\perp \beta B)^5 - \cdots\end{aligned} \tag{15}$$

where $i = 1, 2, 3$ corresponds to the three doublets of the ground manifold mentioned above.

In order to illustrate the high-field effects of the perpendicular transitions qualitatively, we give the solutions for some of the above coefficients:

$$(g_\perp^0)_1 = (g_\perp^0)_2 = 2\sqrt{5}p_0q_0g_J^\perp; \qquad (g_\perp^0)_3 = 3g_J^\perp \tag{16}$$

$$\alpha_1 = \frac{2q_0^2}{E_3^0 - E_1^0} + \frac{5}{4}\frac{(p_0^2 - q_0^2)^2}{E_2^0 - E_1^0} \tag{17}$$

$$\alpha_2 = \frac{2p_0^2}{E_3^0 - E_2^0} + \frac{5}{4}\frac{(p_0^2 - q_0^2)^2}{E_1^0 - E_2^0} \tag{18}$$

$$-\alpha_3 = \alpha_1 + \alpha_2 \tag{19}$$

$$\varepsilon_1^\varphi = \frac{3q_0^2}{(E_1^0 - E_3^0)^2} \tag{20}$$

$$\varepsilon_2^\varphi = \frac{-3p_0^2}{(E_2^0 - E_3^0)^2} \tag{21}$$

$$\varepsilon_3^\varphi = 2\sqrt{5}p_0q_0\left[\frac{p_0^2}{(E_2^0 - E_3^0)} + \frac{q_0^2}{(E_1^0 - E_3^0)}\right]\frac{E_2^0 - E_1^0}{(E_1^0 - E_3^0)(E_2^0 - E_3^0)} = \varepsilon_2 - \varepsilon_1 \tag{22}$$

$$\varepsilon_1 = 2\sqrt{5}p_0q_0\left[-\frac{q_0^2}{(E_1^0 - E_3^0)^2} + \frac{p_0^2 - q_0^2}{(E_1^0 - E_3^0)(E_1^0 - E_2^0)} - \frac{5}{4}\frac{(p_0^2 - q_0^2)^2}{(E_1^0 - E_2^0)^2}\right] \tag{23}$$

$$\varepsilon_2 = 2\sqrt{5}p_0q_0\left[-\frac{p_0^2}{(E_2^0 - E_3^0)^2} + \frac{p_0^2 - q_0^2}{(E_2^0 - E_3^0)(E_1^0 - E_2^0)} - \frac{5}{4}\frac{(p_0^2 - q_0^2)^2}{(E_1^0 - E_2^0)^2}\right] \tag{24}$$

$$\varepsilon_3 = -3\left[\frac{p_0^2}{(E_2^0 - E_3^0)^2} + \frac{q_0^2}{(E_1^0 - E_3^0)^2}\right] = \varepsilon_2^\varphi - \varepsilon_1^\varphi \tag{25}$$

$$\gamma_1^\varphi = \frac{3\sqrt{5}p_0q_0}{(E_2^0 - E_1^0)(E_3^0 - E_1^0)^2}\left[1 - 2q_0^2\left(1 + \frac{E_2^0 - E_1^0}{E_3^0 - E_1^0}\right)\right] \tag{26}$$

$$\eta_1^\varphi = \varepsilon_1^\varphi\left[\frac{(\frac{3}{2})^2 + 15p_0^2q_0^2 - 6q_0^2}{(E_3^0 - E_1^0)^2} + \frac{60p_0^2q_0^2 - 25 + 15q_0^2}{(E_2^0 - E_1^0)^2} + \frac{90p_0^2q_0^2 - \frac{5}{4} - 18p_0^2}{(E_2^0 - E_1^0)(E_3^0 - E_1^0)}\right] + \frac{5}{4}\frac{3\cos 4\varphi}{(E_3^0 - E_1^0)^2(E_2^0 - E_1^0)^2}. \tag{27}$$

At low fields, corresponding to the conventional EPR spectroscopy, the effective g-value of the perpendicular transition given by equation (16) is magnetic-field independent. In our case, the ground doublet and the second excited doublet have the same zero-field effective g-value:

$$(g_\perp^0)_1 = (g_\perp^0)_2 = \sqrt{5}g_J^\perp \frac{|\frac{2C_4}{\Delta C_0}|}{\sqrt{1 + (\frac{2C_4}{\Delta C_0})^2}} = 1.823g_J^\perp = 1.504. \tag{28}$$

If $g_J^\perp$ and $g_J^\parallel$ are considered to have approximately the value of the Landé factor, $(g_\perp^0)_1 = (g_\perp^0)_2$ can be estimated by considering the effective g-value of the parallel-type transition $g_0^\parallel$. At high frequencies and magnetic fields, the effective g-value of the perpendicular-type transitions becomes magnetic-field dependent, because the Zeeman interaction mixes the three doublets of the ground multiplet. Moreover, although $g_x^{\text{eff}}(\varphi = 0) = g_y^{\text{eff}}(\varphi = \frac{\pi}{2})$, the effective value $g_\perp^{\text{eff}}$ shows azimuthal angular dependence. By increasing the frequency and the magnetic field, at the beginning, the most important angular dependence of the line position is in direct ratio with $(g_J^\perp\beta B)^3\varepsilon_i^\varphi \cos 4\varphi$. In the powder spectrum, this dependence splits the line of the perpendicular transition into two lines, one corresponding to $\varphi = 0, \pm\frac{\pi}{2}$, and the other to $\varphi = \pm\frac{\pi}{4}$. In our experiment, the perpendicular transitions are observed only at 95 GHz. These transitions correspond to the ground doublet. Weihe's simulation program shows that the splitting of the perpendicular transition (see figure 3) is due to the azimuthal angular dependence. Thus, the line positions of the two perpendicular transitions may be used to find $g_J^\perp$. The zero-field energy differences among the three doublets of the ground multiplet were found by considering the parallel transitions. They allow us to estimate the orthorhombic distortion from the splitting of the perpendicular transitions. This splitting of 2390 ± 50 G is very well simulated, by considering the orthorhombic distortion to be negligible ($B_2^2 \simeq 0$). In our case, the main contribution of 2195 G comes from the term proportional to ε_1^φ. This contribution is in direct ratio to $(\frac{g_J^\perp\beta B}{E_3^0 - E_1^0})^2(g_J^\perp\beta B)$. Since $p_0^2 \simeq 4q_0^2$, $\varepsilon_3^\varphi, \varepsilon_2^\varphi \gg \varepsilon_1^\varphi$, the splitting of the perpendicular-type transitions corresponding to the two excited doublets must be much larger than that of the ground one. In addition, for these excited doublets, the higher-order contributions proportional to $(g_J^\perp\beta B)^5$, $(g_J^\perp\beta B)^7$, etc are not negligible, and the perturbation treatment ceases to be valid even at 95 GHz. The second splitting must be proportional to $(g_J^\perp\beta B)^5 \cos^2 4\varphi$ (equation (15)). This splitting corresponds to $\varphi = 0, \pm\frac{\pi}{2}, \pm\frac{\pi}{4}$ and $\varphi = \pm\frac{\pi}{8}$. For the ground doublet at 95 GHz it was calculated to be 12 G. The splitting is too small to be measured, but must be appreciable at higher frequencies, or for the two excited doublets.

4. Discussions

The multifrequency HF-EPR powder spectra of trace impurities in GdTrp reported here show that the zero-field splitting of the ground multiplet $^2F_{5/2}$ of Ce^{3+} is comparable with the quanta

of the far-infrared frequencies and with the Zeeman interaction. Therefore, the effective g-values of the EPR transitions between the two levels of the ground doublet show important magnetic-field dependences. For the parallel transition corresponding to tetragonal symmetry, the crystal field and the Zeeman interaction admix only the $|\frac{5}{2}, \pm\frac{5}{2}\rangle$ and $|\frac{5}{2}, \mp\frac{3}{2}\rangle$ states. In this case analytical solutions for the eigenstates and their corresponding eigenvalues can be found. However, in order to explain the magnetic-field dependences of the effective g-value of the parallel transition corresponding to the ground doublet qualitatively, we give the expressions of this value in two limiting cases: (LF)—low field limit $\left(\frac{2g_J^{\parallel}\beta B}{E_2^0-E_1^0}\right)^2 \ll 1$, and (HF)—high field limit $\left(\frac{2g_J^{\parallel}\beta B}{E_2^0-E_1^0}\right)^2 \gg 1$:

$$^{\mathrm{LF}}(g_{\parallel}^{\mathrm{eff}})_1 = g_J^{\parallel}\left\{1 + \frac{4|\Delta C_0|}{E_2^0 - E_1^0}\left[1 - \left(\frac{2g_J^{\parallel}\beta B}{E_2^0 - E_1^0}\right)^2\right] + \cdots\right\}, \tag{29}$$

$$^{\mathrm{HF}}(g_{\parallel}^{\mathrm{eff}})_1 = g_J^{\parallel}\left\{1 + \frac{|\Delta C_0|}{4g_J^{\parallel}\beta B}\left[1 + \frac{1}{2}\left(\frac{E_2^0 - E_1^0}{4g_J^{\parallel}\beta B}\right)^2\right] + \cdots\right\}. \tag{30}$$

By increasing the magnetic-field position of the transition, $g_{\parallel}^{\mathrm{eff}}$ must decrease from the zero-field value $g_J^{\parallel}(1 + \frac{4|\Delta C_0|}{E_2^0-E_1^0})$ to the high-field limit $g_J^{\parallel}$. This decrease is confirmed by our experiment. The line position of the parallel transition corresponding to the ground doublet cannot give any information about the position of the other excited doublet corresponding to the pure $|\frac{5}{2}, \pm\frac{1}{2}\rangle$ states. This information can be retrieved, providing the frequency is sufficiently high, as in our experiment, so that a direct EPR transition between the ground and the above exited doublet can be observed.

The effective g-value of the perpendicular-type transitions depends also on the magnetic field, by increasing the frequency (see equation (15)):

$$(g_{\perp}^{\mathrm{eff}})_i = (g_{\perp}^0)_i + 2g_J^{\perp}(\varepsilon_i + \varepsilon_i^{\varphi}\cos 4\varphi)(g_J^{\perp}\beta B)^2 + 2g_J^{\perp}\left(\eta_i + \eta_i^{\varphi}\cos 4\varphi - \frac{(\varepsilon_i^{\varphi})^2 g_J^{\perp}}{(g_{\perp}^0)_i}\cos^2 4\varphi\right)(g_J^{\perp}\beta B)^4 + \cdots. \tag{31}$$

There are two important differences between the magnetic-field dependences of the effective g-values for the two types of transition. First, contrary to the case of the parallel-type transition (equation (30)), $(g_{\perp}^{\mathrm{eff}})_i$ always depends on the even power of the magnetic field, and second, $(g_{\perp}^{\mathrm{eff}})_i$ also has azimuthal angular dependences. For a symmetry with a twofold axis the last term in the secular equation (14) is proportional to $(g_J^{\perp}\beta B)^2\cos 2\varphi$. This term is responsible for the azimuthal angular dependence of a conventional EPR spectrum with an orthorhombic distortion. This angular dependence is included in the first component of $g_{\perp}^{\mathrm{eff}}$ which is magnetic-field independent. For an axial symmetry with a fourfold axis the last term in equation (14) is proportional to $(g_J^{\perp}\beta B)^4\cos 4\varphi$. The first term of $g_{\perp}^{\mathrm{eff}}$ does not exhibit an angular dependence. However, the terms that are magnetic-field dependent include $\cos^n 4\varphi$ azimuthal angular dependences. For the second term with a square magnetic-field dependence, $n = 1$. In this case the ground multiplet with Kramers degeneracy must have $J \geqslant 5/2$. For a symmetry with a sixfold axis, the secular equation includes a term proportional to $(g_J^{\perp}\beta B)^6\cos 6\varphi$. The first and the second terms in $g_{\perp}^{\mathrm{eff}}$ do not exhibit angular dependence, but the third has a component proportional to $(g_J^{\perp}\beta B)^4\cos 6\varphi$. In this case the ground multiplet with Kramers degeneracy must have $J \geqslant 7/2$, and so on.

For powder spectra of Ce^{3+} with tetragonal symmetry, the azimuthal angular dependence splits the perpendicular transition. For the ground doublet in the GdTrp lattice, this splitting is as a first approximation proportional to $(E_3^0 - E_1^0)^{-2}$ (see equation (20)). Consequently, this

splitting can be used to find the zero-field difference between the doublet corresponding to the pure $|\frac{5}{2}, \pm\frac{1}{2}\rangle$ states and the ground doublet, even when a direct EPR transition between these doublets may not be detectable.

A recent study of the structure of LnTrp complexes [1] suggests that there are two isostructural series of tropolonate complexes. One contains the Sm^{3+}, Tb^{3+}, Dy^{3+}, and Yb^{3+} derivatives that crystallizes in the orthorhombic system. The other contains Er^{3+}, Ho^{3+}, Eu^{3+}, and Gd^{3+} derivatives that crystallizes in the tetragonal system with different cell parameters. The X-band EPR spectrum of Yb^{3+} in YbTrp exhibits a tetragonal symmetry with a small orthorhombic distortion. In contrast, the simulation of the HF-EPR spectra of Ce^{3+} in GdTrp does not detect, within errors, any orthorhombic distortion. So, these two EPR studies confirm the hypothesis of Caneschi *et al* [1] concerning the symmetry in which the Yb^{3+} and Gd^{3+} derivative tropolonate complexes crystallize.

The simulation program shows that the g_J-matrix has two diagonal values, $g_J^z = g_J^{\parallel} = 0.810 \pm 0.005$, and $g_J^x = g_J^y = g_J^{\perp} = 0.825 \pm 0.005$. Both are smaller than the Landé factor for the free ion $g_L = 0.857$. Such small reductions are usual for Ce^{3+} paramagnetic centres [11]. This is because of effects such as: (i) the coupling of different J manifolds by the crystal fields [10], (ii) the covalent reduction of the orbital moment [11], or (iii) the dynamical lowering of the symmetry through lattice vibrations [12]. Since, at low fields, the effective g-values are magnetic-field independent, conventional EPR spectroscopy is not able to show evidence of any anisotropy of the Zeeman interaction. That is because the effective g-values depend not only on the g_J-matrix (see equations (11) and (28)) but also on the crystal-field parameters. In contrast, a multifrequency HF-EPR study allows to find the g_J-matrix separately. The small axial anisotropy measured shows that in our case there is a covalent contribution to the departure of the diagonal g_J-matrix elements from the free-ion value. Since the simulation of the EPR spectra can be made assuming that the ground $J = 5/2$ manifold is well isolated from the excited $J = 7/2$ manifold, we must say that the admixture of the excited manifold has a weak contribution. This admixture could eventually contribute to the small reduction of the diagonal g_J-matrix elements from the free-ion value.

Weihe's program can simulate not only the line positions of the EPR transitions, but also their lineshape and relative intensity. The lineshapes were fitted considering a Lorentzian lineshape for the individual lines of the crystallites due to the relaxation processes, or a Gaussian lineshape due to the dipole–dipole interaction [15]. This fact justifies why the linewidths increase with increasing frequency and temperature [16]. At 285 GHz the individual lineshape of the parallel-type transition is Lorentzian with a linewidth of about $\Delta B_L \simeq 600$ G (see figure 6). In our experiment, at low temperature $\frac{g_{eff}\beta B}{kT} \gg 1$, and the direct spin-lattice relaxation rate T_1^{-1} decreases strongly by decreasing the frequency ($\Delta B_L \sim T_1^{-1} \sim \nu^5$) [3]. As a result of this decrease, at 190 and 95 GHz, the lineshape of the individual lines is mainly Gaussian due to the dipole–dipole interaction between the Ce^{3+} impurity and its Gd^{3+} neighbours. However, the individual linewidth of the parallel-type transitions ($\Delta B_G \simeq 100$ G) is much larger than those of the perpendicular-type transitions $\Delta B_G \simeq 10$ G. The individual lines are also Gaussian distributed because of the spread of the EPR parameters due to lattice imperfections [17]. This is proved by recording the EPR spectra of different powder samples at the same frequency and temperature. These samples have different grain sizes by milling. Figure 2 illustrates that the linewidths of the EPR transitions becomes larger with decreasing grain sizes. As regards the intensity of the transitions, there is a large discrepancy between the intensity of the parallel transitions and the perpendicular transitions. Thus, although the linewidth of the parallel transition at 95 GHz is much larger than those of the perpendicular ones, the intensity of the first-type transition is much larger than those of the second type. By increasing the frequency, this effect increases. This explains why the perpendicular transitions

cannot be observed at 190 GHz, although at this frequency the spectrometer has the best sensitivity, and the parallel-type transition is intense. This striking effect was also observed for Gd^{3+} in the same lattice [2, 6]. It was found [2] that, compared to the calculated powder spectra, the intensity of the central lines of the Gd^{3+} HF-EPR powder spectra were increasingly depleted by increasing the frequency and decreasing the temperature. The central lines are due to Gd^{3+} EPR transitions corresponding to the y-axis that is one of the principal axes of the fine structure tensor. In order to shed light on this H/T effect we performed a detailed lineshape and linewidth analysis of the HF-EPR spectra of GdTrp [6]. We found that the mentioned H/T effect could be explained if the weak dipole spin–spin and the superexchange interactions among the nearest neighbours Gd^{3+} ions are comparable in the crystallographic directions for which these neighbours are situated. The GdTrp structure shows that these directions are the two equivalent binary axes a and b (see figure 1). For the Gd^{3+} spectrum which is strongly orthorhombic, the hypothesis that the y-axis is the a or b axis may be confirmed by performing single-crystal angular dependences. Unfortunately such angular dependences are very difficult to be obtained at low temperatures by our HF-EPR technique. The Ce^{3+} powder spectra exhibit the mentioned H/T effect if the magnetic field is perpendicular to the tetragonal axis c. The Gd^{3+} powder spectra exhibit a similar H/T effect if the magnetic field is along the y-axis. Consequently our hypothesis that the y-axis is one of the two binary axes a or b is correct [6].

5. Conclusions

With the exception of the rare earth ions having $4f^7$ configuration that have a small orbital contribution, many other lanthanide ions with an odd number of electrons have a ground multiplet with $J > 1/2$ and a large orbital contribution. Consequently these paramagnetic ions exhibits a ground doublet and other closed excited doublets. In many cases, the zero-field splitting is too small to be measured by optical spectroscopy, while the susceptibility measurements are not suitable to locate them with a reasonable precision [1]. Conventional microwave EPR spectroscopy usually detects the transitions corresponding to the ground doublet of the J manifold. Therefore, depending on symmetry, there are available only one, two, or a maximum three values of the effective g. These values on one hand are magnetic-field independent, and on the other hand depend on small reductions of the g_J Zeeman interaction factor which can exhibits also a weak anisotropy. It is difficult to determine these adjustable factors and the relevant crystal-field parameters from the observed effective g-values and the normalization relationship because of the uncertainty [18].

However, if the Zeeman interaction is not very small in comparison with the zero-field splitting of the ground manifold, the above effective g-values may exhibit important magnetic-field dependences. Consequently, a multifrequency HF-EPR spectroscopy could be very suitable for determining the zero-field splitting and the adjustable factors of the Zeeman interaction. Moreover, even in axial symmetries, the effective g-factor may exhibit not only a polar angular dependence, but also an azimuthal angular dependence. The azimuthal angular dependence is in the first approximation proportional to $(g_J^{\perp}\beta B)^2 \cos 4\varphi$ for a fourfold axis, $(g_J^{\perp}\beta B)^4 \cos 6\varphi$ for a sixfold axis, etc. The azimuthal angular dependence splits the perpendicular-type transition of the EPR powder spectrum. This splitting may be used to find the zero-field splitting of the ground manifold with a good precision, even if direct transitions between the ground doublet and the excited doublets are not detectable. Consequently, the splitting of the perpendicular transition in a powder HF-EPR spectrum exhibits an important advantage, since it is very difficult to obtain angular dependences on single crystals at high fields and low temperatures.

Acknowledgments

This work was supported by NATO Grant No. PDD(CP)-(PSV.EV 980305). We also gratefully acknowledge financial support from a Short-term Mobility Grant of the Consiglio Nazionale delle Ricerche, Italy. The Access to research Infrastructure action of the Improving Human Potential Program of the European Community is gratefully acknowledged for the Contract No. HPRI-2000-40022 (SENTINEL).

References

[1] Caneschi A, Dei A, Gatteschi D, Poussereau S and Sorace L 2004 *Dalton Trans.* 1048
[2] Caneschi A, Dei A, Gatteschi D, Massa C A, Pardi L A, Poussereau S and Sorace L 2003 *Chem. Phys. Lett.* **371** 69414 and references therein
[3] Abragam A and Bleaney B 1970 *Electron Paramagnetic Resonance of Transition Metal Ions* (Oxford: Clarendon)
[4] Orton J W 1968 *Electron Paramagnetic Resonance: an Introduction to Transition Group Ions in Crystals* (London: ILIFFE Books LTD)
[5] Annino G, Cassettari M, Fittipaldi M, Lenci L, Longo I, Martinelli M, Massa C A and Pardi L A 2000 *Appl. Magn. Reson.* **19** 495
[6] Popescu F F, Martinelli M, Massa C A, Pardi L A and Bercu V 2005 *Magn. Res. Chem* at press
[7] Dong H N, Wu S Y and Zheng W C 2002 *Z. Naturf.* a **57** 753
[8] Rosa J, Asatryan H R and Nikl M 1996 *Phys. Status Solidi* a **158** 573
[9] Yamaga M, Hattori K, Kodama N, Ishizawa N, Honda M, Shimamura K and Fukuda T 2001 *J. Phys.: Condens. Matter* **13** 10811
[10] Elliott J R and Stevens K W H 1952 *Proc. R. Soc.* A **215** 437
[11] Gratens X, Charar S and Averous M 1997 *Phys. Rev.* B **56** 8199
[12] Inoue M 1963 *Phys. Rev. Lett.* **11** 196
[13] Jacobsen C J H, Pedersen E, Villadsen J and Weihe H 1993 *Inorg. Chem.* **32** 1216
[14] Wang Y L and Cooper B R 1970 *Phys. Rev.* B **2** 2607
[15] Bencini A and Gatteschi D 1990 *Electron Paramagnetic Resonance of Exchange Coupled Systems* (Berlin: Springer)
[16] Martinelli M, Massa C A, Pardi L A, Bercu V and Popescu F F 2003 *Phys. Rev.* B **67** 0142251–11
[17] Buzaré J Y, Silly G, Klein J, Scholz G, Stösser R and Nofz M 2002 *J. Phys.: Condens. Matter* **14** 10331
[18] Wingbermuhle J, Meyer M, Schirmer O F, Pankrath R and Kremert R K 2000 *J. Phys.: Condens. Matter* **12** 4277